Photoelectron Spectroscopy and Quantum Chemical Modeling Applied to Polymer Surfaces and Interfaces in Light-Emitting Devices

THOMAS KUGLER,* MIKAEL LÖGDLUND, AND WILLIAM R. SALANECK

Department of Physics, IFM Linköping University, S-581 83 Linköping, Sweden

Received May 12, 1998

Introduction

The work on the doping of free-standing films of polyacetylene to a state of high electrical conductivity by Heeger, MacDiarmid, and Shirakawa in 1977[1] has opened a new field in polymer science.

However, since the discovery[2,3] that poly(*p*-phenylenevinylene), or PPV, and related polymers can be used as the active light-emitting media in polymer-based light-emitting devices,[4−8] interest in conjugated polymers has shifted to their semiconducting properties. In polymer-based light-emitting devices (LEDs), PPV films provide high quantum yields for electroluminescence in the yellow/green portion of the visible spectrum.[5,7,9]

In addition, started by Tang et al.,[10] there is a significant activity in organic molecule based LEDs. The main competition for both organic and polymer LEDs comes from liquid crystals[11] and plasma panels,[12] as well as field-emission displays,[13] all of which are currently ahead technologically for display applications.

The overall quantum efficiency of polymer LEDs is largely determined by the injection of electrons and holes at the respective electrodes.[8,14] Typically, indium−tin oxide coated glass (ITO) is used as the hole-injecting contact. This allows visible light to escape from the active light-generation medium. The counter electrode is usually a metal with a low work function, thereby enabling electron injection into the conduction band of the electroactive polymer. In this context, the investigation of the interaction between conjugated polymer materials and various electrode materials has become an important issue.

This Account reviews the principles involved in the study of the electronic and chemical structure of conjugated polymer surfaces and interfaces. The examples were chosen to illustrate the wide range of information obtainable from photoelectron spectroscopy (PES),[15] both on pristine-conjugated polymers as well as on the modification of the electronic and chemical structure of conjugated systems induced upon interaction with ITO and different metals. Special emphasis is laid on illustrating the usefulness of a combined experimental−theoretical approach, which provides a level of information output larger than the sum of the two parts.[14]

Photoelectron Spectroscopy

Photoelectron spectroscopy (PES) is very useful for studies of the chemical and electronic structure of conjugated polymers and polymer interfaces, because (i) it provides chemical and electronic information within a single technique, (ii) it is essentially nondestructive, and (iii) the method is extremely surface sensitive. PES is carried out by illuminating a sample with light and analyzing the kinetic energy distribution of the photoemitted electrons.

The fundamental process in photoionization of molecules is

$$M_o + h\nu \rightarrow M_+^* + e^- \quad (1)$$

where M_o represents the isolated neutral molecule, $h\nu$ is the ionizing photon, M_+^* represents the positive molecular ion, and e^- is the photoelectron which carries kinetic energy E_k. The energy balance is given by

$$E_o + h\nu = E_+^* + E_k \quad (2)$$

where E_o is the total energy of the neutral molecule in the ground state and E_+^* is the total energy of the positive molecular ion. Thus, the basic equation used in interpreting photoelectron spectra can be written as

$$E_B^V = E_+^* - E_o = h\nu - E_k \quad (3)$$

The photon energy $h\nu$ is known, and the photoelectron kinetic energy distribution is measured in order to deduce the binding energy E_B^V. The binding energy is thus equal to the energy difference between the initial ground-state molecule M_o and the positive molecular ion M_+^*.

The final-state energy of the molecular ion M_+^* is modified by relaxation effects: Intramolecular relaxation occurs in response to the creation of a hole state during

Thomas Kugler, born in 1961 in Friedrichshafen, Germany, studied chemistry at the University of Tübingen, Germany. From 1990 to 1993 he worked on his Ph.D. thesis on organic adsorbates on silicon. In 1994 he joined the Surface Physics and Chemistry group in Linköping, Sweden, as a Postdoctoral Fellow.

Mikael Lögdlund, born in 1959 in Ånge, Sweden, received his Ph.D. at Linköping University, Sweden, in 1993. After a stay as a visiting Postdoctoral Fellow at the Université de Mons-Hainaut in Belgium, he returned to Linköping in 1994, where he presently holds a position as Assistant Professor.

William R. Salaneck, born in 1941 in Pottstown, PA, received his Ph.D. in solid-state physics at the University of Pennsylvania in 1969. After 12 years as a Staff Scientist and 2 years as a Group Manager at Xerox Corporation, he joined Linköping University, Sweden, as Professor of Surface Physics and Chemistry in 1983.

Recent research in the Linköping group has focused upon conjugated organic materials and their interfaces in polymer-based light emitting diodes using photoelectron spectroscopies, quantum chemical calculations, and atomic force microscopy.

10.1021/ar980041o CCC: $18.00
Published on Web 01/29/1999

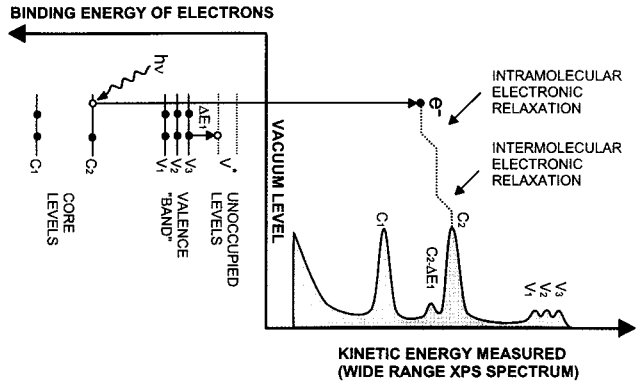

FIGURE 1. Idealized photoelectron spectrum with the corresponding molecular levels (for an explanation, see the text).

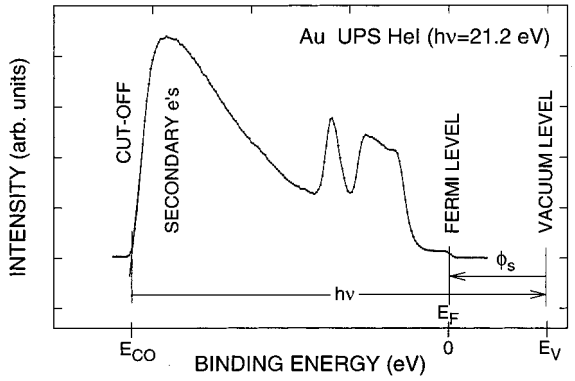

FIGURE 2. Determination of the work function (Φ_s) of a sample (for an explanation, see the text).

photoemission. In the classical picture, the electron leaves the molecule within about 10^{-15} s. The geometry relaxation of the nuclear framework takes around 10^{-13} s, whereas the electronic relaxation time is only about 10^{-16} s.[16] Thus, the electrons have time to relax during the emission process, whereas the nuclear geometry remains frozen. The electronic relaxation energy is given to the escaping electron and increases the kinetic energy.

In the solid state, additional intermolecular relaxation occurs due to the polarization of the surrounding molecules.

Figure 1 displays an idealized photoelectron spectrum with the corresponding molecular levels. Within the one-electron picture, there is a one-to-one correspondence between the peaks in a photoelectron spectrum and the molecular levels in the neutral molecule. The small feature appearing on the low kinetic energy side of the main peak, labeled C_2 in the idealized spectrum, corresponds to a "shake-up" satellite; the escaping electron loses kinetic energy, ΔE_1, as a result of an excitation from an occupied level, V_3, to an unoccupied level, V^*, simultaneously with the electron emission from a core level, C_2.

PES is usually carried out in ultrahigh vacuum (UHV), both for sample surface cleanliness and to reduce the scattering of photoemitted electrons with residual gas molecules. Because of the low kinetic energy of the photogenerated electrons, the technique is surface sensitive, with a nominal interrogation depth varying in the range of about 1−10 nm, depending upon the photon energy.

With XPS, as commonly carried out with Al Kα (1486 eV) and Mg Kα (1254 eV) sources, it is possible to perform a qualitative and even semiquantitative analysis of the chemical composition in the near surface region of a solid sample. Changes in the valence electron density will be reflected as small, but significant shifts in the core level binding energies ("chemical shifts").[17]

The most commonly used laboratory photon source for UPS is the He resonance lamp (He I, 21.2 eV; He II, 40.8 eV), although the use of synchrotron radiation as a photon source is in extensive use today. For valence band spectroscopy, UPS has two advantages over XPS. First, the usual in-house photon sources have high-energy resolution, a full width of half-maximum (fwhm) of ∼30 meV for the He lines, and second, the photoionization cross section for electrons is higher in the valence region for UPS. However, the natural line widths in condensed molecular solids, from both homogeneous and inhomogeneous broadening effects, can approach 1 eV at room temperature,[18,19] thereby reducing the actual energy resolution.

For solid specimens, PES measurements are performed with reference to the Fermi level of the spectrometer. However, in cases where the sample Fermi level shifts due to some chemical modification, e.g., in the doping of conjugated polymers,[20] it is necessary to account for this change before interpreting chemical shifts of spectral features. The change in the Fermi level can be deduced by measuring the position of the cutoff of the secondary electron distribution, as illustrated in Figure 2: The vacuum level is located by adding the photon energy to the secondary electron cutoff energy; measuring down from the vacuum level energy to the position of the Fermi energy (E_F) determines the work function (Φ_s) of the specimen[21] (the position of the Fermi level is determined by performing a UPS measurement on a metallic specimen in equilibrium with the spectrometer[14]).

Valence band spectra provide information about the electronic and chemical structure of the system, since many of the valence electrons participate directly in chemical bonding. To extract this information from the experimental UPS spectra, the spectra are compared to the results of model quantum chemical calculations.[14] This combined experimental−theoretical approach allows for an assignment of the different features in the electronic structure in terms of atomic or molecular orbitals, or in terms of band structure.

Theoretical Approaches

On the basis of Koopman's theorem, the calculated Hartree−Fock eigenvalues of the molecular orbitals in the neutral ground-state molecule are set equal to the binding energies of the photoelectrons.

A common strategy for calculating the density of valence states both for pristine and charged conjugated systems is to use a "two-step procedure": First, the ground-state geometry is optimized using a semiempirical

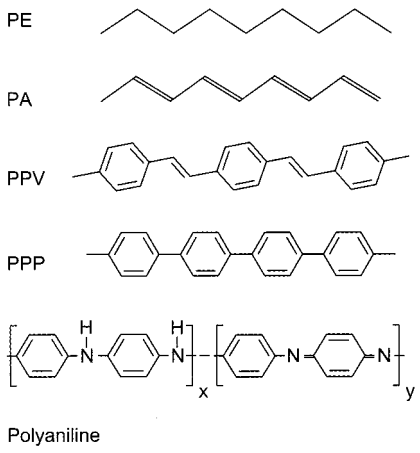

FIGURE 3. The chemical structures of polyacetylene, poly(*p*-phenylenevinylene), poly(*p*-phenylene), and polyaniline. At the top, nonconjugated polyethylene is shown for comparison.

method (for example, modified neglect of diatomic overlap (MNDO)[22] or the Austin model 1 (AM1)[23]). The optimized geometries then serve as the input for electronic structure calculations performed with the nonempirical valence effective Hamiltonian (VEH) pseudopotential method.[24,25] The applicability of the VEH model in interpreting photoelectron valence band spectra of conjugated systems is well established: VEH has an excellent record of providing reliable estimates of ionization potentials, bandwidths, and band gaps for a wide variety of conjugated polymers.[26,27]

Ab initio Hartree−Fock calculations can generate detailed information even in the case of materials involving atoms which are not parametrized within VEH. In addition, density functional theory (DFT) has evolved as a valuable tool because it includes electron correlation effects, which are especially important for the study of polymer interactions with metal atoms, ions, and clusters.[28]

A few of the polymers to which the combined experimental−theoretical approach has been applied[14] are illustrated in Figure 3.

Electronic Structure of Polyacetylene

Due to its simple geometry, polyacetylene (see Figure 3) is particularly suitable for illustrating the relationship between calculated energy band structure and experimental valence band spectra[29] (see Figure 4). To facilitate the comparison between the UPS data and the calculated band structure, the band structure-derived density of valence states, ρ(E) (or DOVS), is included (the energy scale is with respect to the Fermi level in the UPS spectra). The highest occupied energy band is the π-band, which can be seen clearly as the band edge in the UPS spectra.

For discussing energy bands in solids, the molecular orbital eigenvalue problem has to be extended to systems with one-dimensional periodic boundary conditions.[24,25,30] This implies that the solutions of the Schrödinger equation must be of the Bloch form, $\Psi(k,r) = u_k(r)\exp(ikx)$, where

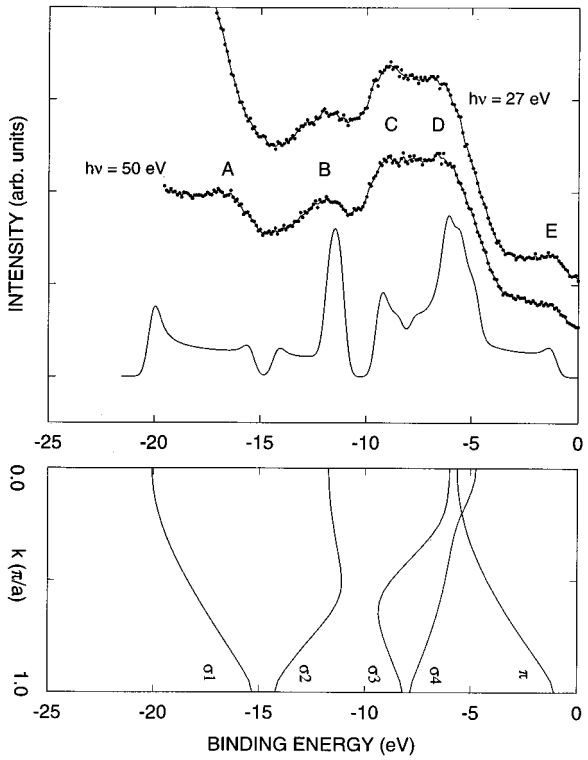

FIGURE 4. Calculated band structure[24,25] and experimental (synchrotron radiation with 27 and 50 eV photon energy) valence band spectra[29] of *trans*-polyacetylene.

$u_k(r)$ has the periodicity of the lattice and k is the crystal momentum along the direction of x. Periodicity in reciprocal space implies that $\Psi(k,r) = \Psi(k+K,r)$, where K is the reciprocal lattice vector. The first Brillouin zone is defined by the region between $-\pi/a \le k \le \pi/a$, where a is the magnitude of the real space lattice vector. The first Bragg reflections and the first forbidden electron energy gap occur at the first Brillouin zone. The electronic band structure of an arbitrary one-dimensional system will contain many overlapping bands, usually of different symmetries, and spread out over different binding energies.

Within this theoretical framework, the electronic structure of *trans*-polyacetylene can be rationalized as follows:[25] If the carbon−carbon bonds were of equal length, the polyacetylene unit cell would consist of a single (−CH−) group, and there would be three occupied valence bands (a C−C σ-band, a C−H σ-band, and a π-band derived from the remaining p_z atomic orbital on each C-atom). The π-band would be only half-filled, and the polymer would be metallic. However, the system dimerizes (Peierls transition), forming alternating single and double bonds, which results in a unit cell containing two carbon atoms (−CH═CHunit). Since the width of the one-dimensional Brillouin zone is now only half of that for the regular polyene, each band of the regular polyene splits into two bands, resulting in four occupied σ-bands and one fully occupied π-band. Energy gaps occur at the Brillouin zone edge, near −8 and −15 eV in Figure 4, where each (regular polyene structure) band is folded back to form the dimerized-chain band

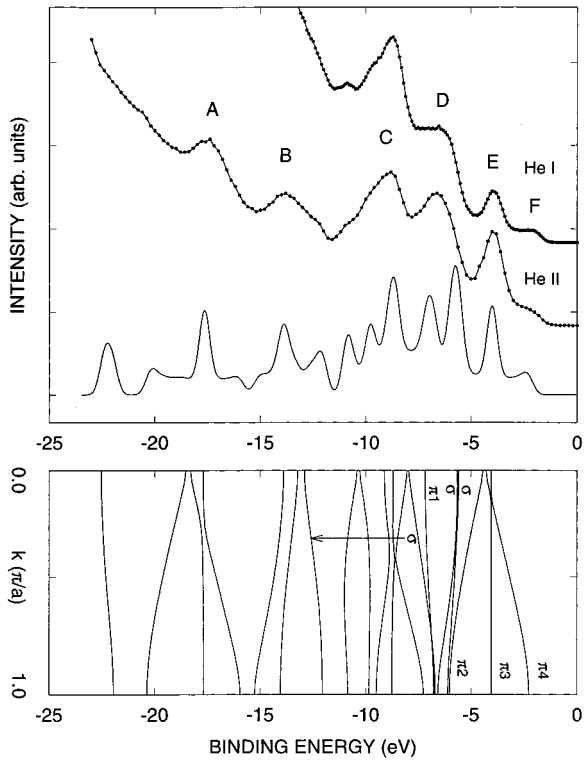

FIGURE 5. He I and He II valence band spectra of PPV compared with VEH-derived DOVS (VEH band structure in the lower part of the figure).

structure. The Peierls gap in the π-band, which occurs at the Brillouin zone edge, corresponds to an energy gap of approximately 1.5 eV.

Electronic Structure of Poly(*p*-phenylenevinylene)

The electronic structure of poly(*p*-phenylenevinylene) (PPV) is illustrated in Figure 5, where UPS spectra are compared with the results of a VEH band structure calculation. The excellent agreement between experiment and theory can be seen, especially at lower binding energies in the so-called frontier electronic structure region (certain discrepancies are to be expected as neither photoionization cross-sections nor many-body effects, which mostly affect the inner valence region of the valence band in hydrocarbons, are included in the theoretical results). The density of valence states shown in direct comparison with the UPS spectra is obtained from the band structure displayed at the bottom of Figure 5. The frontier electronic structure is displayed at the right of the figure: it is composed of the p-band edge and a more intense peak, corresponding to the dispersionless flat band localized on the phenyl groups (near −4 eV).

In studying the interaction of metal atoms with the surface of PPV (as discussed below), the frontier electronic structure changes in specific ways, depending upon the nature of the interaction between metal atoms and the polymer surface.

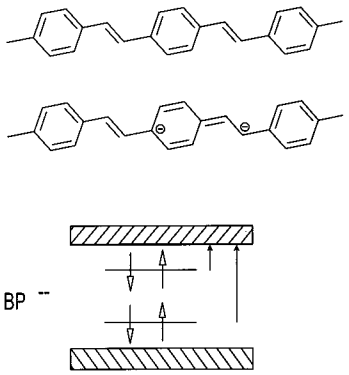

FIGURE 6. Band diagram of negative bipolarons (BP^{--}) in PPV.

Metals on Poly(*p*-phenylenevinylene)

In the many reports on PES studies of the interface formation between PPVs and metals, the main focus is on the two most commonly used top electrode metals in polymer light-emitting device structures, namely, aluminum[31−34] and calcium.[34−36] Other metals studied include chromium,[37] gold,[38] nickel,[38] sodium,[39] and rubidium.[40]

After the charge carriers encountered upon doping of PPV are introduced in the following section, results from various PES studies of the interaction of PPV with sodium and calcium will be discussed in more detail.

Charge Carriers in Poly(*p*-phenylenevinylene). The general property of conjugated organic molecules that the geometric structure is dependent upon the charge on the molecule (strong electron (hole)−lattice interactions), leads to the existence of unusual charge-carrying species. These species manifest themselves as self-localized electronic states within the otherwise forbidden electron energy gap.[41−43]

In the case of a nondegenerate ground-state polymer such as PPV, the very first single electron on any isolated polymer chain goes in as a polaron. However, the individual polarons then combine to form spinless bipolarons, thus achieving a lower energy configuration.[41−44] The negatively charged bipolaron states for PPV are sketched in Figure 6.

Sodium on Poly(*p*-phenylenevinylene). The behavior of sodium atoms on the surface of PPV was studied by Fahlman et al.[45] The UPS spectra indicate a slight decrease in the work function as the first monolayer equivalents of sodium are deposited on the surface, while, according to XPS, the sodium atoms diffuse uniformly throughout the polymer film. At about 40% doping, a large decrease in the work function (about 1.2 eV) occurs, followed by a slight decrease as the doping level approaches 100%, i.e., one sodium atom per "monomer" repeat unit. Simultaneous with the 1.2 eV change in the work function, two new states appear in the previous HOMO-to-LUMO gap. Their intensities increase uniformly with the doping level (Figure 7).[45] The separation between the two doping-induced peaks is about 2.0 eV at the maximum doping level (near 100%), with the lower binding energy peak

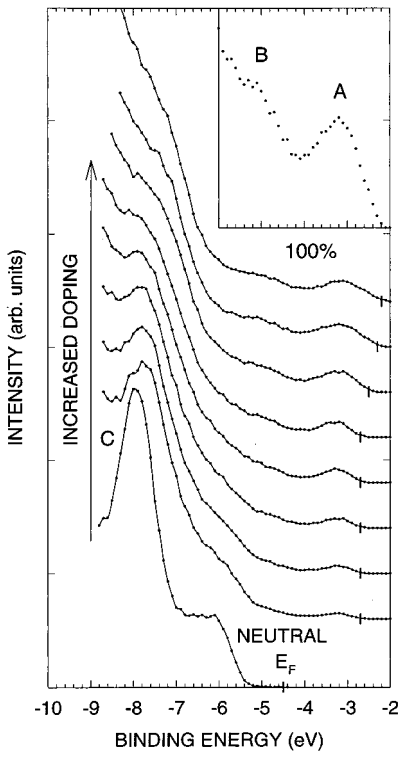

FIGURE 7. Low binding energy part of the He I spectra of PPV as a function of successive exposures to sodium atoms.[45]

positioned at about −3.2 eV. From model VEH calculations, the new states appearing in the previously forbidden energy gap are assigned to two doping-induced bipolaron bands. Experimentally, the lack of any density of states at the Fermi level, as would occur for polaron bands, indicates the formation of bipolarons.

This bipolaron signature in UPS will be used in the studies described next to identify the nature of the interaction of calcium atoms with PPV. This topic is of considerable interest, since calcium electrodes are often used in fabricating polymer-based LEDs.

Calcium on Poly(*p*-phenylenevinylene). Observed clearly first for DP7,[46] and subsequently for DHPPV,[36] calcium diffuses into the near surface region of a PPV film, donates electrons to the polymer π-system, and forms Ca^{2+}-ions. The interfacial region between the Ca-metal contact and the polymer scales in the range of 20−40 Å. These results arise from a detailed combined theory−experiment study of the behavior of calcium atoms on the surface and in the near surface region of ultrathin films of clean PPV in UHV.[14]

In contrast to the case of clean PPV, when there are large numbers of oxygen-containing species at the surface of PPV[47] or substituted PPVs,[46] an interfacial layer of calcium oxide is formed initially, followed by the deposition of calcium metal after the oxygen-containing species have been consumed. The scale of this interfacial oxide layer depends on the details of the surface contamination, chemical impurity of the polymer, and/or the vapor-deposition environment.

The combined results of a variety of published studies on calcium electrodes on PPV are summarized[48,49] in

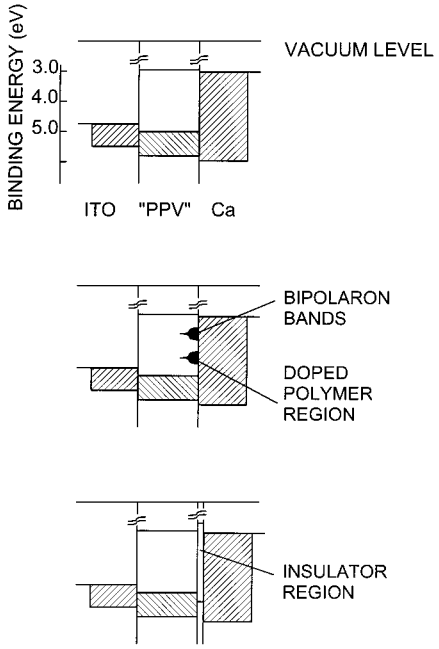

FIGURE 8. Model interfacial energy band situations pertaining to the nature of the interfacial surface region in PPV.[48]

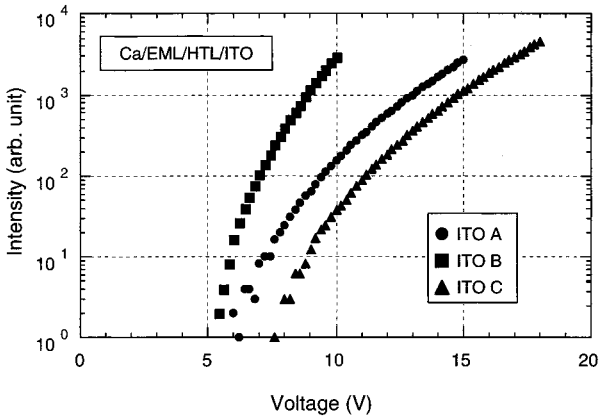

FIGURE 9. I vs V curves for devices made from three different types of ITO with almost identical work functions:[57] emitting layer (EML), MEH−PPV; hole transport layer (HTL), poly (*N*-vinylcarbazole).

Figure 8, where the ideal-interface model is shown at the top, and the two extremes are shown at the bottom: doped bipolaron states in the near surface region for the case of clean calcium on clean PPVs,[36,46] and the calcium "oxide" interfacial layer, in the case of calcium on PPV with a high density of oxygen-containing species on the surface.[47]

Implications for the Optimization of Metal Electrodes in Polymer LEDs. To study the effect of the presence of oxygen-containing species during vapor deposition of the metal electrode, LEDs consisting of a calcium electrode on a single polymer film on ITO glass were prepared using spectroscopically clean PPV films.[50] The vapor deposition of the calcium electrodes was carried out in the presence of a varying oxygen background pressure, ranging from less than 10^{-12} to 10^{-4} mbar in (otherwise) UHV. It was found that, considering factors such as device yield, performance lifetime, and initial luminescence intensity, an optimum occurs for about 10^{-6} mbar of O_2 background

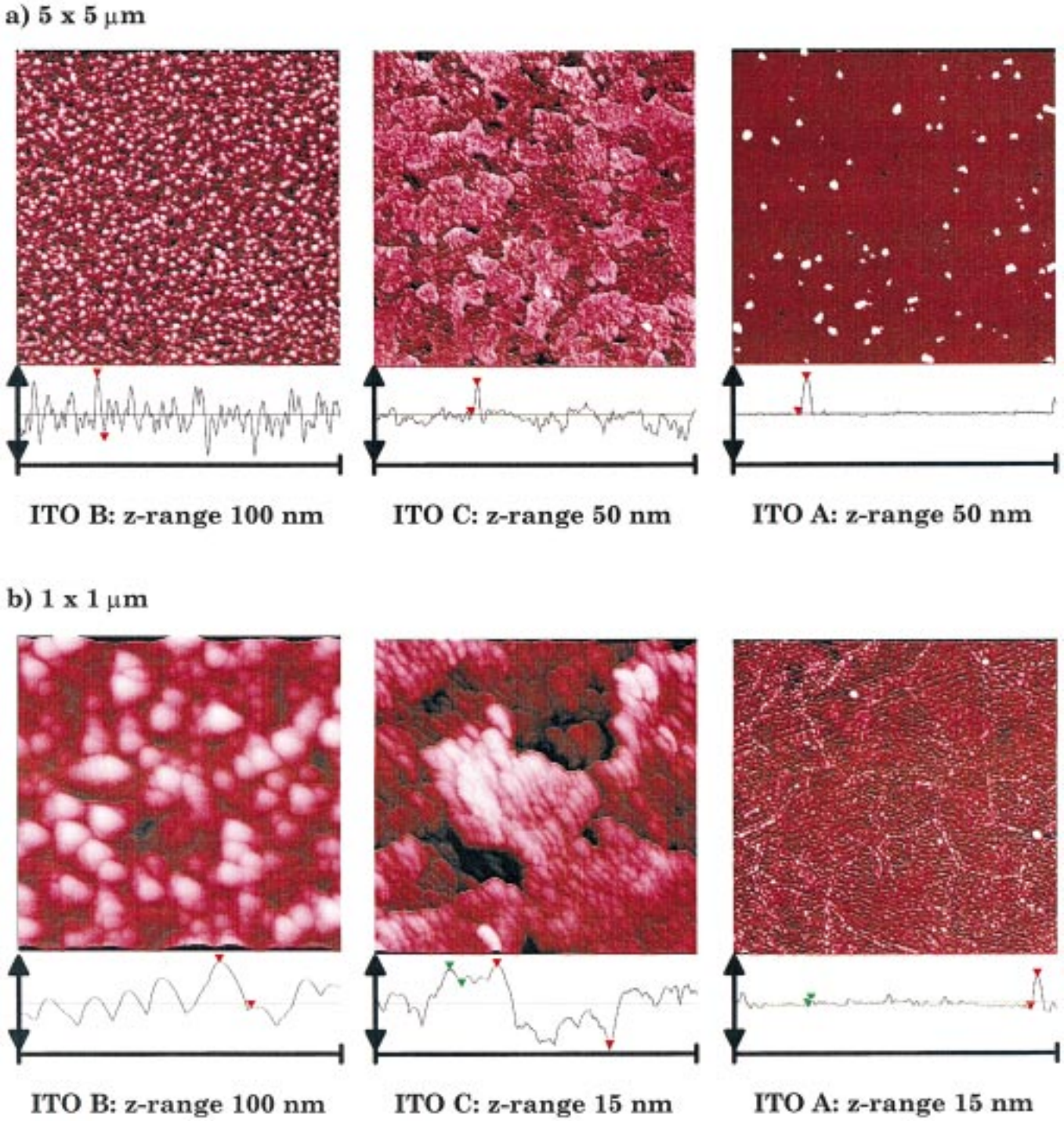

FIGURE 10. Tapping-mode AFM images (top) and cross-sections (bottom) of three different types of ITO. Scan sizes: (a) 5 × 5 μm, (b) 1 × 1 μm.[57]

pressure. Without knowing the precise chemical composition of the "dirty calcium" electrodes described above, it appears that the presence of partly oxidized calcium is not detrimental but actually provides "better" devices.[50]

Other studies revealed metal-induced emission quenching as an explanation for poor performance in certain configurations.[51] The fact that, in the case of metal-induced emission quenching, the emission can be recovered by intentional partial oxidation of the metal (calcium in particular)[52] is consistent with the calcium issues discussed above.

The ITO Electrode in Polymer LEDs

Recent reports indicated that the ITO electrode chemically interacts with electroactive polymers, leading to a loss of conjugation through the formation of carbonyl species. However, it is possible to stabilize the chemistry of the electrode−polymer interface by coating the ITO anode

with doped polyaniline: In addition to a higher current and brighter emission, the polyaniline injection layer lowers the rate of degradation as compared to uncoated ITO.[53] The lower operating voltage and increased quantum efficiency of the devices using polyaniline-coated ITO as compared to devices using ITO alone as the hole-injecting anode[54] were attributed to a higher electronegativity of doped polyaniline as compared to ITO, thus providing a smaller barrier to hole injection into MEH−PPV.[55] Other systems studied as hole-injecting buffer layers between the ITO electrode and the emissive layer in organic LEDs include the doped form of a polythiophene derivative (PEDOT/PSS).[56]

To study the influence of substrate precleaning on the performance of LEDs, devices were fabricated and characterized in UHV, as discussed previously,[50] using MEH−PPV as the emitting layer and three different types of ITO, denominated A, B, and C.[57,58] Despite the fact that all three ITO samples had almost identical work functions (4.7−4.8 eV), the turn-on voltages for light emission are clearly different (see Figure 9). Obviously, the ITO work function is not the only factor in determining the hole-injection characteristics at the ITO−polymer interface.

In this context, it is important to note the strong differences in surface morphology, which is an important parameter influencing the local electric field distribution at the respective ITO−polymer interfaces. Figure 10 displays 5 × 5 μm and 1 × 1 μm tapping-mode AFM pictures of three hydrogen peroxide treated ITO samples, B, C, and A (arranged in order of decreasing surface roughness σ_{RMS}): ITO B, which produced the lowest turn-on voltage, displays a granular structure resulting in a very rough surface (σ_{RMS} = 15.6 nm). ITO C has a flakelike surface (see Figure 10a; σ_{RMS} = 2.7 nm), with the flakes displaying a granular internal structure (see Figure 10b). ITO A displays an extremely flat surface decorated with isolated protrusions (see Figure 10a; σ_{RMS} = 1.6 nm). Zooming in to the flat areas between these protrusions, tiny droplets can be seen (see Figure 10b; σ_{RMS} within the flat areas = 0.4 nm).[57]

In addition to the work function and surface roughness, additional factors such as chemical interactions at the polymer−ITO interface are expected to influence the hole-injection characteristics of the ITO−polymer interface. In the following, initial results on the chemical interactions of two different polyaniline oligomers with clean ITO A surfaces will be presented.

Interactions of Polyaniline Oligomers with ITO. The interaction of polyaniline with ITO was studied using oligomeric model compounds (phenyl-capped amino (PC2) and imino (PC2OX) dimers; see Figure 11), allowing the interactions of the amino and imino functionalities in polyaniline with ITO to be studied separately. Reference spectra of both model compounds were obtained from thick films. As the thickness of the organic layer was then decreased, details of the oligomer−ITO interface appeared.

XPS Results. A series of N(1s) core level spectra for the imino compound are shown in Figure 12. In the case of

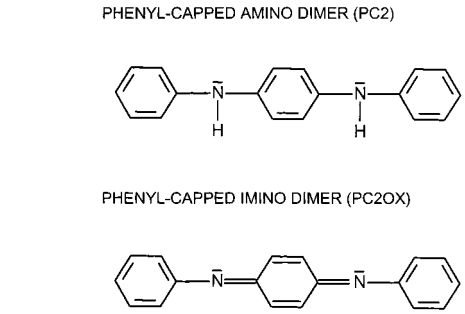

FIGURE 11. Polyaniline model compounds PC2 and PC2OX.

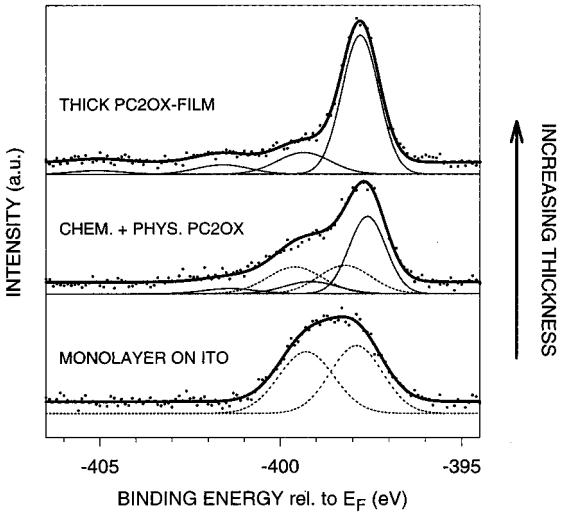

FIGURE 12. N(1s) core level spectra of PC2OX on ITO: upper curve, thick film; central curve, intermediate film; lower curve, ultrathin film (monolayer); bold solid lines, fitted curves; thin solid and dotted lines, Gaussian peak components for physisorbed and chemisorbed PC2OX, respectively.

the thick PC2OX film, the N(1s) emission contains a main component at 397.8 eV, together with some shake-up peaks. Decreasing film thickness leads to a broadening toward higher binding energy, finally resulting in a symmetric N(1s) emission composed of the original component (slightly shifted to 397.9 eV) and an additional, high binding energy component at 399.3 eV. This indicates an interaction between one of the two imino nitrogens in each molecule and the ITO surface, whereas the second imino nitrogen apparently does not interact.[59] In the corresponding series of spectra for the amino model compound, the N(1s) emission remains essentially unchanged at a binding energy of 398.9 eV, except for a small increase of the fwhm (not shown here).

UPS Results. UPS spectra for a series of increasingly thinner layers of the amino compound (PC2) on ITO are shown in Figure 13. In the case of the thick PC2 film, the low binding energy electronic structure displays clearly resolved peaks at −5.8, −6.9, −8.1, and −9.1 eV (denominated as A, B, C, and D). Decreasing the film thickness results in a gradual merging of peaks A and B, resulting in a broad, unstructured shoulder in the limit of the chemisorbed monolayer. A deeper insight into the specific chemical interactions within the adsorbed monolayer can be obtained by comparing the experimental UPS spectra

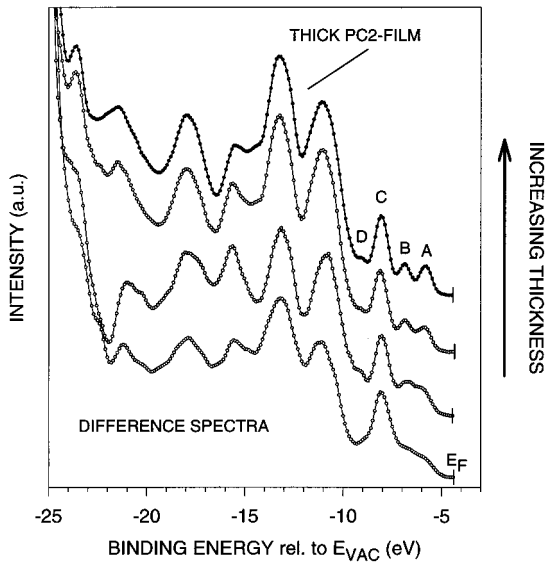

FIGURE 13. He II spectra of PC2 on ITO: uppermost curve (filled dots), thick PC2 film; other curves (empty dots), difference spectra between increasingly thinner PC2 films on ITO and clean ITO; lower curve, monolayer.

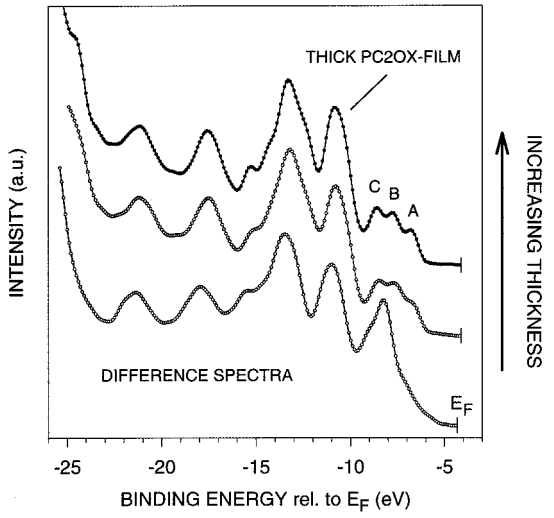

FIGURE 14. He II spectra of PC2OX on ITO: uppermost curve (filled dots), thick PC2OX film; other curves (empty dots), difference spectra between increasingly thinner PC2OX films on ITO and clean ITO; lower curve, monolayer.

to the results of DFT calculations on both an isolated PC2 molecule and a PC2 molecule interacting with an $In(OH)_3$-$(OH_2)_2$ cluster representing the ITO surface:[59] Whereas the LUMO of the model adsorbate is mostly In5s-derived, the HOMO displays a strong contribution from one of the nitrogen lone pairs. This indicates a donor−acceptor-type interaction between one of the amino nitrogens of the PC2 molecule and an indium cation on the ITO surface.

More drastic changes in the electronic structure are observed for the imino compound (PC2OX) upon interaction with ITO. For the thick PC2OX film, we observe clearly resolved peaks in the low binding energy range at −6.8, −7.8, and −8.6 eV (denominated as A, B, and C in Figure 14). In the limit of the chemisorbed monolayer, however, this structure is completely changed, forming a broad peak at 8.2 eV tailing toward low binding energy. Together with the splitting of the N(1s) emission observed in XPS, this result clearly indicates a strong interaction of the imino groups with the ITO surface.

Summary

Some details of the electronic structure of specific metal-on-polymer and polyaniline oligomer-on-ITO interfaces have been presented to illustrate the importance of such interfaces in determining device performance in polymer LEDs. In every instance studied, there is always some chemistry that occurs at the interface. There is no such thing as an ideal metal−polymer contact without interfacial chemistry of one sort or another. In this context, it is clear that the ultimate control of the interface will be one of the major determining steps in the exploitation of reliable polymer-based electronic devices.

This work was supported by the European Commission through a TMR Network (Project Number 1354 SELOA), as well as by a contract with Hoechst A.B. Research on conjugated polymers in Linköping is supported in general by grants from the Swedish Natural Sciences Research Council (NFR), the Swedish Research Council for Engineering Sciences (TFR), and the Swedish National Board for Industrial and Technical Development (NuTek).

References

(1) Chiang, C. K.; Fincher, C. R.; Park, Y. W.; Heeger, A. J.; Shirakawa, H.; Louis, E. J.; Gao, S. C.; MacDiarmid, A. G. Electrical conductivity in doped polyacetylene. *Phys. Rev. Lett.* **1977**, *39*, 1098−1101.

(2) Burroughes, J. H.; Bradley, D. D. C.; Brown, A. R.; Marks, R. N.; Mackay, K.; Friend, R. H.; Burn, P. L.; Holmes, A. B. Light emitting diodes based upon conjugated polymers. *Nature* **1990**, *347*, 539−541.

(3) Friend, R. H. Semiconductor devices fabricated with conjugated polymers: novel optoelectronic properties. In *Nobel Symposium in Chemistry: Conjugated Polymers and Related Materials; The Interconnection of Chemical and Electronic Structure*; Salaneck, W. R., Lundström, I., Rånby, B., Eds.; Oxford Science: Oxford, 1993; pp 285−323.

(4) Braun, D.; Heeger, A. J. Visible light emission from semiconducting polymer diodes. *Appl. Phys. Lett.* **1991**, *58*, 1982−1984.

(5) Burn, P. L.; Holmes, A. B.; Kraft, A.; Bradley, D. D. C.; Brown, A. R.; Friend, R. H. Synthesis of a segmented conjugated polymer chain giving a blue-shifted electroluminescence and improved efficiency. *J. Chem. Soc., Chem. Commun.* **1992**, 32−36.

(6) Grem, G.; Leditzky, G.; Ullrich, B.; Leising, G. Realization of a blue-light-emitting device using poly(*p*-phenylene). *Adv. Mater.* **1992**, *4*, 36−37.

(7) Halliday, D. A.; Burn, P. L.; Bradley, D. D. C.; Friend, R. H.; Gelsen, O. M.; Holmes, A. B.; Kraft, A.; Martens, J. H. F.; Pichler, K. Large changes in optical response through chemical pre-ordering of poly(*p*-phenylenevinylene). *Adv. Mater.* **1993**, *5*, 40−43.

(8) Parker, I. D. Carrier tunneling and device characteristics in polymer light-emitting diodes. *J. Appl. Phys.* **1994**, *75*, 1656−1666.

(9) Gymer, R. W.; Friend, R. H.; Holmes, A. B.; Staring, E. G. J.; Marks, R. N.; Taliani, C.; Bradley, D. D. C.; Dos Santos, D. A.; Bredas, J. L.; Lögdlund, M.; Salaneck, W. R. Conjugated polymer electroluminescence − Review for Nature. *Nature*, in press.

(10) Tang, C. W.; VanSlyke, S. A. Organic Electroluminescent diodes. *Appl. Phys. Lett.* **1987**, *51*, 913−915.
(11) Bahadur, B. *Liquid Crystals: Applications and Uses*; World Scientific: Singapore, 1997; Vols. 1−3.
(12) Deschamps, J. Color Display Panels. *16th International Display Research Conference*; SID: Birmingham, U.K., 1996.
(13) Gomer, R. *Field Emission and Field Ionization*; AIP: New York, 1993.
(14) Salaneck, W. R.; Stafström, S.; Brédas, J. L. *Conjugated Polymer Surfaces and Interfaces*; Cambridge University Press: Cambridge, 1996.
(15) *Polymer Surfaces*; Clark, D. T., Feast, W. J., Eds.; John Wiley & Sons: Chichester, 1978.
(16) Fadley, C. S. Basic concepts of X-ray photoelectron spectroscopy. In *Electron Spectroscopy: Theory, Techniques and Applications*; Brundle, C. R., Baker, A. D., Eds.; Academic Press: London, 1978; p 1.
(17) Siegbahn, K.; Nordling, C.; Johansson, G.; Hedman, J.; Heden, P. F.; Hamrin, V.; Gelius, U.; Bergmark, T.; Werme, L. O.; Manne, R.; Baer, Y. *ESCA Applied to Free Molecules*; North-Holland: Amsterdam, 1971.
(18) Duke, C. B.; Salaneck, W. R.; Fabish, T. J.; Ritsko, J. J.; Thomas, H. R.; Paton, A. The Electronic Structure of Pendant-Group Polymers: Molecular Ion States and Dielectric Properties of Poly (2-Vinyl Pyridine). *Phys. Rev.* **1978**, *B18*, 5717−5739.
(19) Salaneck, W. R. Photoelectron spectroscopy of the valence electronic structure of polymers. *CRC Crit. Rev. Solid State Mater. Sci.* **1985**, *12*, 267−296.
(20) Salaneck, W. R.; Erlandsson, R.; Prejza, J.; Lundström, I.; Inganäs, O. X-ray photoelectron spectroscopy of boron fluoride doped polymer. *Synth. Met.* **1983**, *5*, 125−139.
(21) Plummer, E. W.; Eberhardt, W. Angle-resolved photoemission as a tool for the study of surfaces. In *Advances in Chemical Physics*; Prigogine, I., Rice, S. A., Eds.; John Wiley & Sons: New York, 1982; Vol. 49, p 533.
(22) Dewar, M. J. S.; Thiel, W. Ground states of molecules. 39. MNDO results for molecules containing Hydrogen, Carbon, Nitrogen and Oxygen. *J. Am. Chem. Soc.* **1977**, *99*, 4907−4917.
(23) Dewar, M. J. S.; Zoebisch, E. G.; Healy, E. F.; Stewart, J. J. P. AM1: A new general purpose quantum mechanical molecular model. *J. Am. Chem. Soc.* **1985**, *107*, 3902−3909.
(24) Brédas, J. L.; Chance, R. R.; Silbey, R.; Nicolas, G.; Durand, P. A nonempirical effective Hamiltonian technique for polymers: application to polyacetylene and polydiacetylene. *J. Chem. Phys.* **1981**, *75*, 255−267.
(25) André, J. M.; Delhalle, J.; Brédas, J. L. *Quantum Chemistry Aided Design of Organic Polymers*; World Scientific: Singapore, 1991.
(26) Brédas, J. L.; Salaneck, W. R. Electronic-Structure Evolution Upon Thermal Treatment Of Polyacrylonitrile: A Theoretical Investigation. *J. Chem. Phys.* **1986**, *85*, 2219−2226.
(27) Orti, E.; Brédas, J. L. Photoelectron spectra of phthalocyanine thin films: A valence band theoretical interpretation. *J. Am. Chem. Soc.* **1992**, *114*, 8669−8675.
(28) Fredriksson, C.; Brédas, J. L. Metal/conjugated polymer interfaces: a theoretical investigation of the interaction between aluminum and trans-polyacetylene oligomers. *J. Chem. Phys.* **1993**, *98*, 4253−4262.
(29) Lögdlund, M.; Salaneck, W. R.; Meyers, F.; Brédas, J. L.; Arbuckle, G. A.; Friend, R.; Holmes, A. B.; Froyer, G. The Evolution of the Electronic Structure in a Conjugated Polymer Series: Polyacetylene, Poly(*p*-phenylene), and Poly(*p*-phenylenevinylene). *Macromolecules* **1993**, *26*, 3815−3820.
(30) Kittel, C. *Introduction to Solid State Physics*; John Wiley & Sons: New York, 1986.
(31) Dannetun, P.; Lögdlund, M.; Salaneck, W. R.; Fredriksson, C.; Stafström, S.; Holmes, A. B.; Brown, A.; Graham, S.; Friend, R. H.; Lhost, O. New results on metal−polymer interfaces. *Mol. Cryst. Liq. Cryst.* **1993**, *228*, 43−48.
(32) Konstadinidis, K.; Papadimitrakopoulos, F.; Galvin, M.; Opila, R. L. In situ X-ray photoelectron spectroscopy study of aluminum/poly(*p*-phenylenevinylene) interfaces. *J. Appl. Phys.* **1995**, *77*, 5642−5646.
(33) Nguyen, T. P.; Mansot, J. L. Metal−oxygen−carbon interaction in the poly(*p*-phenylene vinylene)-aluminum system: a study by analytical transmission electron microscopy and X-ray photoelectron spectroscopy. *Thin Solid Films* **1996**, *283*, 135−139.
(34) Hsieh, B. R.; Ettedgui, E.; Gao, Y. The surface species of poly(*p*-phenylene vinylene) and their effects on metal interface formation. *Synth. Met.* **1996**, *78*, 269−275.
(35) Gao, Y.; Park, K. T.; Hsieh, B. R. Interface formation of Ca with poly(*p*-phenylene vinylene). *J. Appl. Phys.* **1993**, *73*, 7894−7899.
(36) Dannetun, P.; Fahlman, M.; Fauquet, C.; Kaerijama, K.; Sonoda, Y.; Lazzaroni, R.; Brédas, J. L.; Salaneck, W. R. Interface formation between poly(2,5-diheptyl-*p*-phenylenevinylene) and calcium: Implications for light emitting diodes. In *Organic Materials for Electronics: Conjugated Polymer Interfaces with Metals and Semiconductors*; Brédas, J. L., Salaneck, W. R., Wegner, G., Eds.; North-Holland: Amsterdam, 1994; pp 133−136.
(37) Nguyen, T. P.; Jonnard, P.; Vergand, F.; Staub, P. F.; Thirion, J.; Lapkowski, M.; Tran, V. H. Characterization of the poly(para-phenylene vinylene)-chromium interface by attenuated total reflection infrared and X-ray emission spectroscopies. *Synth. Met.* **1995**, *75*, 175−179.
(38) Nguyen, T. P.; de Vos, S. Interfacial effects in poly (*p*-phenylene-vinylene)-metal systems. *Vacuum* **1996**, *47*, 1153−1158.
(39) Fahlman, M.; Bröms, P.; dos Santos, D. A.; Moratti, S. C.; Johansson, N.; Xing, K.; Friend, R. H.; Holmes, A. B.; Brédas, J. L.; Salaneck, W. R. Electronic structure of pristine and sodium-doped cyano-substituted poly(2,5-dihexyloxy-*p*-phenylenevinylene): a combined experimental and theoretical study. *J. Chem. Phys.* **1995**, *102*, 8167−8174.
(40) Iucci, G.; Xing, K.; Lögdlund, M.; Fahlman, M.; Salaneck, W. R. Polaron to bipolaron transition in a conjugated polymer. Rubidium-doped poly(*p*-phenylenevinylene). *Chem. Phys. Lett.* **1995**, *244*, 139−144.
(41) Rice, M. J. Charged π-phase kinks in lightly doped polyacetylene. *Phys. Lett.* **1979**, *71*, 152−154.
(42) Su, W. P.; Schieffer, J. R.; Heeger, A. J. Solitons in polyacetylene. *Phys. Rev. Lett.* **1979**, *42*, 1698−1701.
(43) Heeger, A. J.; Kivelson, S.; Schrieffer, J. R.; Su, W.-P. Solitons in conducting polymers. *Rev. Mod. Phys.* **1988**, *60*, 781−850.
(44) Brédas, J. L.; Chance, R. R.; Silbey, R. Comparative theoretical study of the doping of conjugated polymers: polarons in polyacetylene and polyparaphenylene. *Phys. Rev. B* **1982**, *26*, 5843−5854.

(45) Fahlman, M.; Beljonne, D.; Lögdlund, M.; Burn, P. L.; Holmes, A. B.; Friend, R. H.; Brédas, J. L.; Salaneck, W. R. Experimental and theoretical studies of the electronic structure of Na-doped poly(*p*-phenylenevinylene). *Chem. Phys. Lett.* **1993**, *214*, 327−332.
(46) Dannetun, P. Private communication.
(47) Gao, Y.; Park, K. T.; Hsieh, B. R. X-ray photoemission investigations of the interface formation of Ca and poly(*p*-phenylenevinylene). *J. Chem. Phys.* **1992**, *97*, 6991−6993.
(48) Salaneck, W. R.; Brédas, J. L. The metal-on-polymer interface in polymer light emitting diodes. *Adv. Mater.* **1996**, *8*, 48−52.
(49) Salaneck, W. R.; Bredas, J. L. Conjugated polymer surfaces and interfaces for light-emitting devices. *Bull. Mater. Res. Soc.* **1997**, *22*, 46−51.
(50) Bröms, P.; Birgersson, J.; Johansson, N.; Lögdlund, M.; Salaneck, W. R. Calcium electrodes in polymer LEDs. *Synth. Met.* **1995**, *74*, 179−181.
(51) Choong, V. E.; Park, Y.; Gao, Y.; Wehrmeister, T.; Mullen, K.; Hsieh, B. R.; Tang, C. W. Dramatic photoluminescence quenching of phenylene vinylene oligomer thin films upon submonolayer Ca deposition. *Appl. Phys. Lett.* **1996**, *69*, 1492−1494.
(52) Park, Y.; Choong, V. E.; Hsieh, B. R.; Tang, C. W.; Gao, Y. Gap-state induced photoluminescence quenching of phenylene vinylene oligomer and its recovery by oxidation. *Phys. Rev. Lett.* **1997**, *78*, 3955−3958.
(53) Scott, J. C.; Kaufman, J. H.; Brock, P. J.; DiPietro, R.; Salem, J.; Goitia, J. A. Degradation and failure of MEH−PPV light-emitting diodes. *J. Appl. Phys.* **1996**, *79*, 2745−2751.
(54) Yang, Y.; Heeger, A. J. Polyaniline bilayer composite electrode for efficient polymer light emitting diodes. *Mol. Cryst. Liq. Cryst.* **1994**, *256*, 537−542.
(55) Heeger, A. J.; Parker, I. D.; Yang, Y. Carrier injection into semiconducting polymers: Fowler-Nordheim field-emission tunneling. *Synth. Met.* **1994**, *67*, 23−29.
(56) Scott, J. C.; Carter, S. A.; Karg, S.; Angelopoulos, M. Polymeric anodes for organic light-emitting diodes. *Synth. Met.* **1997**, *85*, 1197−1200.
(57) Kugler, T.; Johansson, Å.; Dalsegg, I.; Gelius, U.; Salaneck, W. R. Electronic and chemical structure of conjugated polymer surfaces and interfaces: applications in polymer-based light emitting devices. *Synth. Met.* **1997**, *91*, 143−146.
(58) Osada, T.; Kugler, T.; Bröms, P.; Salaneck, W. R. Polymer-Based Light Emitting Devices: Investigations On The Role Of The Indium Tin Oxide Electrode. *Synth. Met.* **1998**, *96*, 77−80.
(59) Kugler, T.; Salaneck, W. R. Photoelectron spectroscopy studies of the polyaniline-ITO-interface. To be published.

AR980041O